

# Modelling of Solar Thermal Electricity Plants in the POSYTYF Research Project for an Extensive Integration of Renewable Energy Sources

Lourdes González <sup>1</sup>[\[https://orcid.org/0000-0001-6140-3258\]](https://orcid.org/0000-0001-6140-3258), Mario Biencinto <sup>1</sup>[\[https://orcid.org/0000-0003-1757-9584\]](https://orcid.org/0000-0003-1757-9584),  
Loreto Valenzuela <sup>2</sup>[\[https://orcid.org/0000-0001-9505-8333\]](https://orcid.org/0000-0001-9505-8333), Luis Arribas <sup>3</sup>[\[https://orcid.org/0000-0002-1418-2138\]](https://orcid.org/0000-0002-1418-2138),  
and Jesús Polo <sup>3</sup>[\[https://orcid.org/0000-0003-2431-2773\]](https://orcid.org/0000-0003-2431-2773)

<sup>1</sup> Ciemat-Plataforma Solar de Almería, Avda. Complutense 40, 28040 Madrid (Spain).

<sup>2</sup> Ciemat-Plataforma Solar de Almería, Ctra. de Senés km 4.5, 04200 Tabernas, Almería (Spain).

<sup>3</sup> Ciemat, Avda. Complutense 40, 28040 Madrid (Spain).

**Abstract.** This article presents a simplified simulation model of a concentrated solar thermal power plant developed in the framework of the European research project POSYTYF (POWering SYstem flexibiliTY in the Future through RES). Increasing the share of Renewable Energy Sources (RES) in modern power grids is of critical importance for the transformation of the energy markets worldwide. However, the stability of the grid and the limited participation in ancillary services of RES limit their use, especially when high penetration is expected from them. A solution to overcome these issues is to increase the share of so-called dispatchable RES (hydropower, biomass, concentrating solar thermal power). The main objective of the POSYTYF project is to group several renewable and non-renewable energy sources into a Dynamic Virtual Power Plant (DVPP). The simplified simulation model of a parabolic-trough solar thermal power plant developed consists of sub-models for the solar field, thermal energy storage system and power block and it has been validated with real DNI profiles and production data of a commercial STE plant in Spain. The differences between the simulation and real data of daily net production for the days analysed are lower than 1%.

**Keywords:** Solar Thermal Electricity Plant Simulation Model, Parabolic Trough, Thermal Energy Storage, Renewable Energy Sources, Dynamic Virtual Power Plant, Grid Integration.

## Introduction

The European Union (EU) is on track to meet its target of at least 32% renewable energy share in 2030 and two thirds in 2050 set in the new revised Renewables energy directive (2018/2001) and the EU SET Plan [1]. Increasing the share of Renewable Energy Sources (RES) in modern power grids is of critical importance for the transformation of the global energy system. However, the stability of the grid and the limited participation in ancillary services of RES limit their use, especially when high penetration is expected from them. A solution to overcome these issues is to increase the share of so-called dispatchable RES, i.e. the ones that have energy storage capacity (hydropower, biomass, concentrating solar thermal power). The main objective of this project is to group several renewable and non-renewable energy sources into a Dynamic Virtual Power Plant (DVPP). DVPP is a way to aggregate dispatchable/non-dispatchable RES in such a way that resources can be managed internally, in an optimal way in case of meteorological or electrical system variations, in order to provide sufficient flexibility, reliable power output and grid services. The paper is structured as follows: first, objectives, components and scenarios of the DVPP are explained, and later on, the simulation model of a solar

thermal electricity plant, used in the simulation of DVPP, is described and results and their validation are presented.

## Dynamic Virtual Power Plant (DVPP)

The main idea in POSYTYF project is to group several RES into a Virtual Power Plant (VPP), which allows safe operation. The VPP concept facilitates the integration of RES generators with the grid by offering their combined flexibility, internally balancing their fluctuations, and selling their aggregate generation output on the wholesale market. This notion was already used in Spain, for the secondary frequency-power control [2], [3]. In this project, it is extended into a new concept, called Dynamic Virtual Power Plant (DVPP) (Figure 1) in which will jointly address static power dispatch, at single VPP level and dynamic coordination of several VPPs to provide ancillary services to the system, all economically optimized [4].

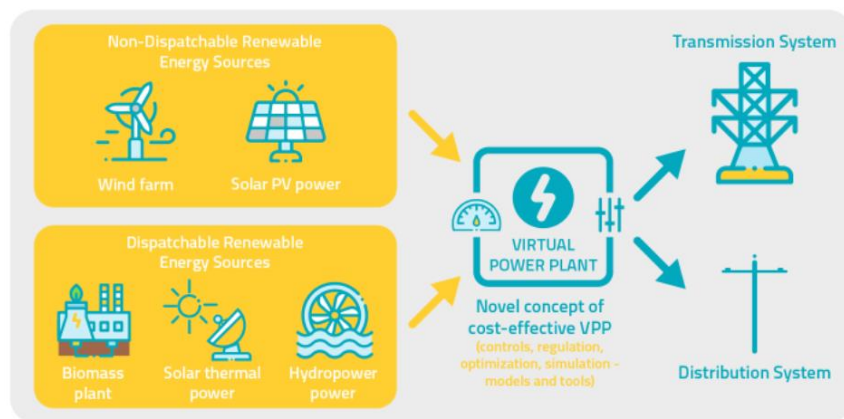


Figure 1. DVPP concept.

The DVPP proposed in this work thus appears as a promising approach to overcome the limitations of electrochemical energy storage systems (battery) and as a competitive solution to increase the viability of non-dispatchable RESs.

### Objective, components and scenarios

The main objective of the DVPP is to integrate a set of RES (dispatchable and non-dispatchable), which allows to provide, to the electrical system, energy in a flexible way and that can participate in auxiliary services.

This DVPP aims to group together some renewable sources, both dispatchable and non-dispatchable, which allows an optimal internal management of resources. DVPP generators can be geographically spread so they are not necessarily close one to each other. Conversely, some RES generators can be close to other dynamic elements of the grid that do not belong to the DVPP.

The main RES generators of the DVPP considered in this study are large-scale power plants as solar photovoltaic, concentrated solar thermal plants, including thermal energy storage in molten salts, offshore and onshore wind plants, pumped-storage hydropower with bidirectional operation and hydropower plants, biomass and geothermal plants.

Conventional thermal units already existing can also be considered and integrated in the DVPP, such as CF-TPS coal-fired thermal power station, CC-TPS combined-cycle thermal

power station and N-TPS nuclear thermal power station. Additional units like batteries, hydrogen electrolyser, flexible loads, etc. can also be added to the DVPP.

From the point of view of the electrical grid, different configurations and options must be taken into account:

- **Continental and island power systems:** the DVPP can insert a set of RES in an interconnected power system or in an isolated island. In the first case, it will participate to existing control schemes for the large thermal plants. In the second case, it will directly ensure voltage and frequency services.
- **Transmission and distribution grids:** RES can be connected on both transmission and distribution sides. The new DVPP concept should allow participation of RES generators from both sides. This implies coordination of the control actions through both grids. This coordination is intended at both administrative (share of the data/measures and control actions) and technical (different voltage levels and different structure of the grids) levels.
- **Several grid connection points:** insertion of the DVPP in the rest of the system may be via several connection points. Moreover, the DVPP may have RES generators in several distribution grids.
- **Imbricated structure:** RES generators included into the DVPP are not chosen from geographical or topological considerations. As a consequence, components of a DVPP are not necessarily neighbours. Moreover, some neighbour generators may not participate to the DVPP.

Considering all the previous information and to reduce the number of possible combinations, three typical scenarios have been selected.

- Type I: **islanded scenarios** are in general smaller and simpler as compared to continental scenarios (e.g. Canary Islands, Spain).
- Type II: the vast majority of scenarios are **synchronously interconnected (AC)** systems, and they are typically bigger and more meshed. Therefore, a higher number of buses and different voltage levels (e.g. transmission and distribution) are considered. Two different versions of this type of scenario are considered. One corresponds to a typical scenario with good solar resource (e.g. South Italy), whereas the other corresponds to a typical scenario with good onshore and offshore wind resource, including HVDC interconnected offshore wind (e.g. west Denmark scenario).
- Type III: **non-synchronously interconnected (HVDC)** scenarios without AC interconnections, they typically correspond to bigger islands. For that reason, the grid layout considered is slightly more complex, with a higher number of buses as compared to Type I. In addition, different voltage levels are also considered in this case (e.g. Corsica and Sardinia scenario, Mediterranean Sea).

To achieve the final objectives of this project, different simulation models of RES technologies have been developed, including a solar thermal power plant with parabolic trough collectors, which is widely described in the following section.

## Solar Thermal Electricity (STE) plant simulation model

A “quasi-dynamic” model of STE plant has been developed in MATLAB by means of m-file functions. The STE plant considered in the simulation model is an Andasol-type solar power plant [5] of 55 MW<sub>e</sub> gross electric output. This type of solar power station includes a Solar Field (SF) with parabolic-trough collectors, a 2-tank Thermal Energy Storage (TES) system with molten salts as heat storage medium and a Power Block (PB) based on a steam Rankine cycle (Figure 2). The main typical features of each subsystem of the STE plant are the following:

- **Solar Field (SF):** 160 loops of parabolic-trough collectors with 4 or 6 collectors per loop (depending on collector length), using thermal oil (diphenyl oxide/biphenyl, e.g. Therminol® VP1) as heat transfer fluid (HTF); with mass flow rates between 300 and 1400 kg/s and with nominal HTF temperatures at the outlet and the inlet of the solar field of 391 °C and 298 °C, respectively.
- **Thermal Energy Storage (TES):** two-tank system (hot & cold tanks at temperatures 386 & 292 °C, respectively) with molten nitrate salts (Solar Salt) as storage medium, and an oil-salt HX. It represents a storage capacity between 7-9 h (900-1300 MWh<sub>t</sub> ≈ 350-500 MWh<sub>e</sub>).
- **Power Block (PB):** includes a steam generation train (with preheater, steam generator, superheater and reheater), a steam turbine, a wet-cooling condenser and a synchronous generator of 55 MW<sub>e</sub> gross power (around 50 MW<sub>e</sub> net power).

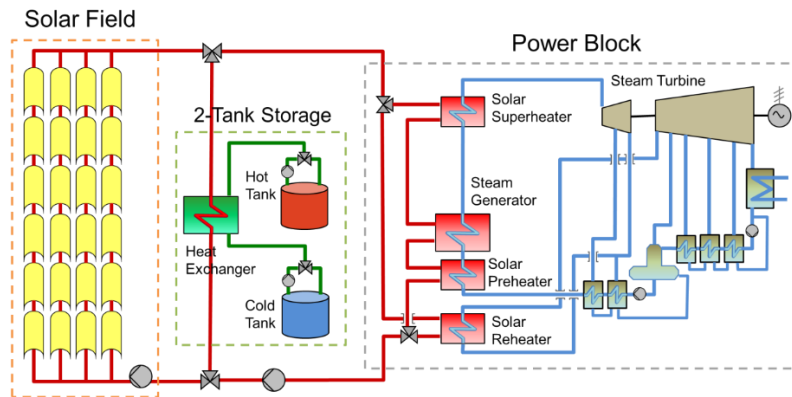


**Figure 2.** Diagram and subsystems of the solar thermal electricity plant to be simulated.

## Model description and formulation

This model simulates steady-state, cloud transient conditions, startup and shutdown processes, by mean of expressions that reproduce the effect of thermal inertia, with time steps from 1 to 10 minutes. The input data of the simulation model for each time step are: direct normal irradiance (DNI), ambient temperature and load to PB. The model allows setting initial values of storage load, PB state, temperatures and mass flows. The output data are gross and net power, storage load, inlet/outlet SF temperatures, mass flows, etc. The configuration of the model enables the adjustment of plant parameters such as SF loops, temperature set-points, reference mass flow rates, parasitic consumptions, etc.

A diagram of the STE plant with the main variables to be computed and their calculation flow is depicted in Figure 3.

First, the net thermal power gained by the fluid in the SF,  $Q_{net,,}$ , is evaluated with a thermal energy balance between solar power absorbed by the collectors and heat losses to the environment ( $Q_{loss,SF}$ ):

$$Q_{net,,} = \eta_{opt,0^\circ} \eta_{sh} \eta_{clean} K(\theta) G_{bn} \cos(\theta) A_{net,SF} - Q_{loss,SF} \quad (1)$$

Where  $G_{bn}$  is the direct normal solar irradiance,  $A_{net,SF}$  is the net collection area,  $\theta$  is the incidence angle of the direct solar radiation on the collector aperture plane,  $K(\theta)$  is the incidence angle modifier,  $\eta_{opt,0^\circ}$  is the peak optical efficiency of the solar collectors,  $\eta_{clean}$  corresponds to the cleanliness factor and  $\eta_{sh}$  represents the shadowing factor.

The expression for the incidence angle modifier  $K(\theta)$  of parabolic troughs is taken from the experimental characterization of EuroTrough-II collectors [6]. The heat losses in the SF,

$Q_{loss,i}$ , are evaluated with an equation obtained from outdoor tests for standard PTR<sup>®</sup>70 receiver tubes [7].

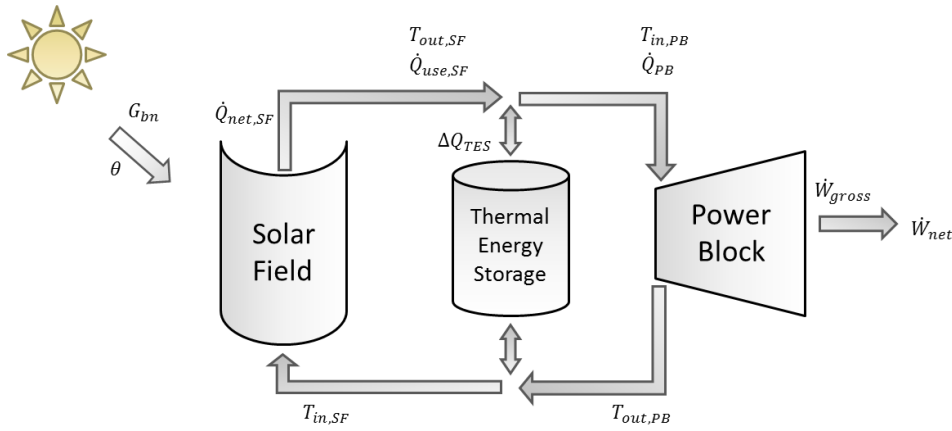


**Figure 3.** Simplified diagram of the STE plant model and main variables considered.

The outlet temperature of the SF in steady-state conditions,  $T_{out,SF,\infty}$ , can be obtained applying a simplified thermal energy balance as follows:

$$T_{out,\infty} = T_{in,SF} + Q_{net,SF} / (\dot{m}_{SF} \cdot c_p) \quad (2)$$

Where  $T_{in,SF}$  is the temperature at the inlet,  $c_p$  is the specific heat of the HTF and  $\dot{m}_{SF}$  is the mass flow rate in the SF. The mass flow rate is obtained with the same thermal energy balance presented in eq. (2) but using the set-point or reference outlet temperature of the SF for  $T_{out,SF,\infty}$ .

In order to incorporate thermal inertia with a simplified approach, a differential equation can be applied to approximate the energy balance in the SF for transient conditions:

$$Q_{net} = C_{ef,SF} dT_{out,SF}/dt + \dot{m}_{SF} \cdot c_p \cdot (T_{out,SF} - T_{in,SF}) \quad (3)$$

The coefficient  $C_{ef,SF}$  represents an effective thermal capacity that depends on the total mass of fluid and pipe in the SF and the specific operating conditions regarding flow and temperature. Eq. (3) corresponds to a 1<sup>st</sup> order linear differential equation with constant coefficients whose solution is an exponential expression that is applied to calculate the SF outlet temperature:

$$T_{out,SF} = T_{out,SF,\infty} + (T_{out,SF,old} - T_{out,SF,\infty}) \cdot \exp(-\dot{m}_{SF} \cdot c_p \cdot \Delta t / C_{ef,SF}) \quad (4)$$

Where  $\Delta t$  is the time step of the simulation, in seconds, and  $T_{out,SF,old}$  the outlet temperature in the previous step. As a result, the actual useful thermal power considering thermal inertia is obtained by applying the outlet temperature from eq. (4):

$$Q_{use} = \dot{m}_{SF} \cdot c_p \cdot (T_{out,SF} - T_{in,SF}) \quad (5)$$

The change in thermal energy stored in the TES system in a time step  $\Delta t$  is computed with:

$$\Delta Q_{TES} = (Q_{use,SF} - Q_{PB}) \cdot \Delta t \quad (6)$$

When the useful thermal power from the SF is higher than the thermal power ( $Q_{PB}$ ) sent to the PB, then  $\Delta Q_{TES} > 0$  and the remaining heat is used to charge the TES system. Otherwise,  $\Delta Q_{TES} < 0$  and then the TES system is discharged to feed the PB.

The specific thermal power to be sent to the PB,  $Q_{PB}$ , is determined at each moment by the desired PB load, which can be either introduced as an additional input to the model or

established according to a standard operation strategy. For instance, a common strategy applied in many STE plants is to reach almost 100% load when the fluid comes from the SF or around 80% load when it comes from the TES system. The gross electric power is then obtained from the thermal power sent to the PB:

$$W_{gross} = \eta_{max, PB} \eta_{load} \eta_{Tin} Q_{PB} \quad (7)$$

Where  $\eta_{max, PB}$  is the maximum gross efficiency of the PB;  $\eta_{load}$  and  $\eta_{Tin}$  are efficiency factors calculated with the following expressions depending on the thermal load ( $load_{PB,t} = Q_{PB}/Q_{max, PB}$ ) or the inlet temperature to the PB:

$$\eta_{load} = 1.0775 - 0.0813/load_{PB,t} + 0.003777/load_{PB,t}^2 \quad (8)$$

$$\eta_{Tin} = (T_{in, PB}/T_{in, PB, ref}) \cdot (T_{in, PB, ref} + 273) / (T_{in, PB} + 273) \quad (9)$$

In eq. (9),  $T_{in, PB}$  is the actual PB inlet HTF temperature, whereas  $T_{in, PB, ref}$  represents its nominal value. In fact,  $\eta_{Tin}$  represents a relation between those temperatures in Celsius and in absolute units. As seen in eq. (9), both variables are considered in absolute units by adding 273 K to their values in °C.

The outlet temperature of the heat transfer fluid from the PB in steady-state conditions (in °C) is calculated with:

$$T_{out,} = 193.6 + 105 \cdot load_{PB,t} + 65 \cdot load_{PB,t} \cdot F_{Tin, PB} - 24 \cdot F_{Tin, PB}^2 \quad (10)$$

Where  $F_{Tin, PB}$  is a factor that measures the relative proximity of the PB inlet temperature to its reference value:  $F_{Tin, PB} = (T_{in, PB, ref} - T_{in, PB}) / (T_{out, PB, ref} - T_{in, PB, ref})$ . Equations (8)-(10) have been obtained by adjusting real curves of a commercial STE plant [8]. Besides, the inlet temperature for the SF and the PB for transient conditions are calculated including thermal inertia with a similar approach to that described by eq. (4).

The net electric power is obtained by subtracting parasitic losses from the gross electric power:

$$W_{net} = W_{gross} - W_{loss} \quad (11)$$

Parasitic losses (kW) include fixed and variable electric losses and pumping consumptions, and are calculated with:

$$W_{loss} = W_{pump} + 1600 + 120 \cdot F_{oper,} + 1400 \cdot \max(F_{oper, SF}, F_{oper, PB}) + 1000 \cdot load_{PB,e}^2 + 200 \cdot load_{SF}^2 \quad (12)$$

Where  $W_{pump}$  includes pumping consumptions in the SF, the TES system and the PB, which are calculated with a simple cubic relation, based on pump affinity laws [9], as function of the mass flow rate through each subsystem ( $W_{pump} = F_{pump} \cdot m^3$ ). The rest of terms in eq. (12) depend on the PB electric load ( $load_{PB,e} = W_{gross}/W_{max}$ ), the SF thermal load ( $load_{SF} = Q_{use, SF}/Q_{max, SF}$ ) and whether the SF or the PB are in operation. Factors  $F_{oper, SF}$  and  $F_{oper, PB}$  take the value 1 when the SF or the PB are running, respectively, or 0 otherwise. The specific coefficients of eq. (12) have been adjusted using real production data from commercial STE plants.

Table 1 gathers the typical features and default parameters considered for the simplified STE plant model.

**Table 1.** Main parameters considered in the simplified model of the STE plant.

Parameters	value
Working fluid in receiver tubes	Therminol® VP-1

Type of solar collector	EuroTrough
Peak optical efficiency (%)	76.8
Cleanliness factor of the mirrors (%)	97
Net collection area of the SF (m <sup>2</sup> )	524800
Nominal temperature at SF outlet / PB inlet (°C)	391
Nominal temperature at SF inlet / PB outlet (°C)	298
Fluid in the 2-tank TES	Solar Salt (60% NaNO <sub>3</sub> /40%KNO <sub>3</sub> )
Capacity of the 2-tank TES (MWh <sub>t</sub> )	1300
Effective thermal capacity of the SF (MJ/K)	1500...3000
Maximum gross efficiency of the PB (%)	39.5
Maximum thermal power from the SF (MW <sub>t</sub> )	320
Maximum gross electric power (MW <sub>e</sub> )	55

## Model validation

The simplified model of STE plant has been validated by comparing the simulation results with real DNI profiles and production data of a commercial STE plant in Spain, which are restricted data. Three representative days have been chosen for the validation: a partly cloudy day near the spring equinox, 24th March 2018, and two sunny days near the summer and winter solstices, 8th July 2018 and 9th December 2018. The time steps of the meteorological data available for these days are 1, 5 and 10 min, respectively. Since the simulation step considered is 1 min, missing DNI values have been interpolated. Figure 4 depicts the results of net electric power of the real plant, and obtained from the simulation, together with the measured DNI for each day.

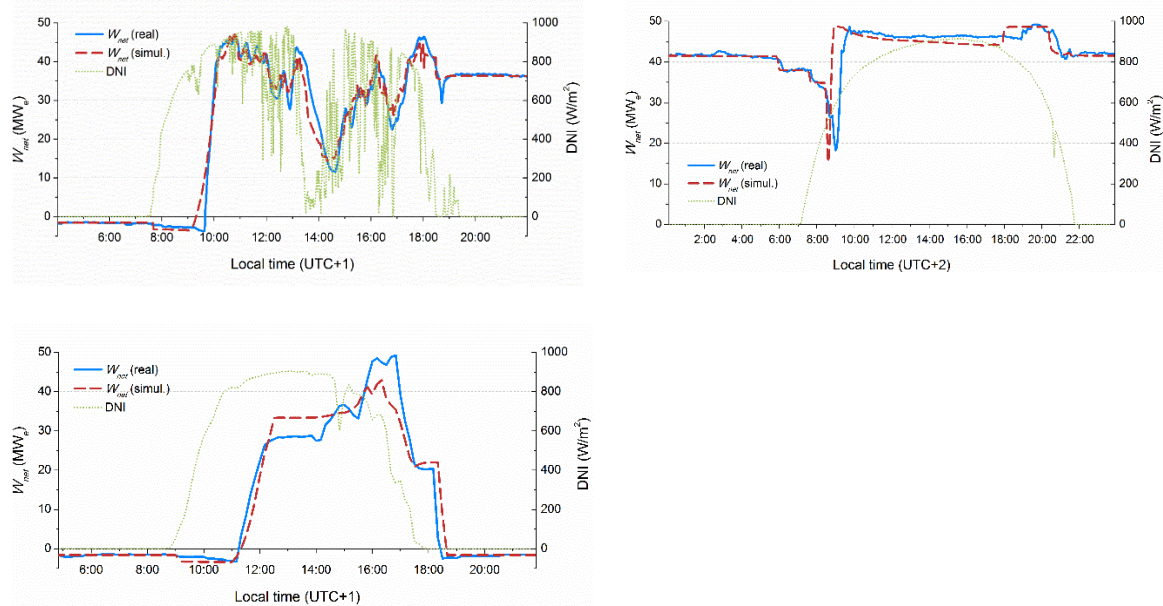


**Figure 4.** Net electric power generated by a commercial STE plant and obtained from the simulation model, including measured DNI, for three representative days: (up left) 24th March 2018, (up right) 8th July 2018 and (down left) 9th December 2018.

A good agreement is observed between the real data and the simulation results. Considering only the period with positive net production, the root mean squared error in terms of net electric power is 3.0 MW<sub>e</sub> for 24th March 2018, 4.0 MW<sub>e</sub> for 8th July 2018 and 6.0 MW<sub>e</sub> for 9th December 2018. The daily net electricity actually obtained at the plant was 478.7 MWh<sub>e</sub>, 1033.7 MWh<sub>e</sub> and 183.8 MWh<sub>e</sub>, respectively, whereas for the same cases the simulation yields 477.8 MWh<sub>e</sub>, 1032.2 MWh<sub>e</sub> and 182.5 MWh<sub>e</sub>. The resulting differences in daily net production

for the days analysed, always lower than 1%, can be considered accurate enough for the scope of this model.

## Competing interests

The authors declare no competing interests.

## Acknowledgement

The research work leading to this article received funds from the EU within the framework of the Horizon 2020 POSYTYF project (Grant Agreement 883985).

## References

1. European Commission, “Energy roadmap 2050,” Luxembourg: Publications Office of the European Union, 2012.
2. E.L. Miguelez, I.E. Cortes, L. Rouco, G.L. Camino, “An overview of ancillary services in Spain”, in *Electric Power Systems Research*, Vol. 78 (2008) pp. 515–523.
3. I. Egido, F. Fernández-Bernal, L. Rouco, Member, “The Spanish AGC System: Description and Analysis”, in *IEEE TRANSACTIONS ON POWER SYSTEMS*, VOL. 24 (2009) NO. 1, FEBRUARY
4. B. Marinescu, O. Gomis-Bellmunt, F. Dörfler, H. Schulte, L. Sigrist. “Dynamic Virtual Power Plant: a new concept for grid integration of renewable energy sources”. *arXiv:2108.00153 [cs, eess]*, July 2021. arXiv: 2108.00153.
5. Solar Millenium, The parabolic trough power plants Andasol 1 to 3. <http://large.stanford.edu/publications/power/references/docs/Andasol1-3engl.pdf>, 2008 (accessed 10 November 2021).
6. M. Geyer, E. Lüpfert, R. Osuna, A. Esteban, W. Schiel, A. Schweitzer, E. Zarza, P. Nava, J. Langenkamp, E. Mandelberg, “EUROTROUGH – Parabolic Trough Collector Developed for Cost Efficient Solar Power Generation”, in: *Proceedings of the 11th SolarPACES International Conference*, 4–6 September 2002, Zurich, Switzerland, 2002.
7. L. Valenzuela, R. López-Martín, E. Zarza, “Optical and thermal performance of large-size parabolic-trough solar collectors from outdoor experiments: A test method and a case study”. In *Energy* 70 (2014) pp. 456–464.
8. Siemens Energy, Industrial Steam Turbines. <https://www.siemens-energy.com/global/en/offering/power-generation/steam-turbines/industrial-steam-turbines.html>, 2021 (accessed 8 November 2021).
9. M. Stewart, “Centrifugal Pumps”, in: *Surface Production Operations: Volume IV - Pump and Compressor Systems: Mechanical Design and Specification*, Gulf Professional Publishing, 2018, pp. 61-309, ISBN 978-0-12-809895-0.